International Journal of Cardiology xxx (2014) xxx–xxx

Contents lists available at ScienceDirect

International Journal of Cardiology

journal homepage: www.elsevier.com/locate/ijcard

Dynamic assessment of the changing geometry of the mitral apparatus in 3D could stratify abnormalities in functional mitral regurgitation and potentially guide therapy

Qing-shan Lin [a,1], Fang Fang [a,1], Cheuk-man Yu [a,1], Yan-Chao Zhang [a,1], Ming C. Hsiung [b,1], Ivan S. Salgo [c,1], Jen-Li Looi [a,1], Song Wan [d,1], Randolph H.L. Wong [d,1], Malcom J. Underwood [d,1], Jun-Ping Sun [a,1], Wei-Hsian Yin [d,1], Jeng Wei [d,1], Chun-na Jin [a,1], Shen-Kou Tsai [d,1], Ling Ji [a,1], Alex Pui-Wai Lee [a,*,1]

[a] *Institute of Vascular Medicine, The Chinese University of Hong Kong, Hong Kong*
[b] *Division of Cardiology, Heart Center, Cheng-Hsin General Hospital, Faculty of Medicine, National Yang-Ming University, Taipei, Taiwan*
[c] *Philips Healthcare, Andover, MA, United States*
[d] *Division of Cardiothoracic Surgery, Department of Surgery, Prince of Wales Hospital, The Chinese University of Hong Kong, Hong Kong*

ARTICLE INFO

Article history:
Received 8 January 2014
Received in revised form 7 July 2014
Accepted 2 August 2014
Available online xxxx

Keywords:
Real-time 3-dimensional transesophageal echocardiography
Functional mitral regurgitation
Tenting volume

ABSTRACT

Introduction: In functional mitral regurgitation (FMR), effective regurgitant orifice area (EROA) displays a dynamic pattern. The impact of dynamic changes of annulus dysfunction and leaflets tenting on phasic EROA was explored with real-time three-dimensional transesophageal echocardiography (RT3D-TEE).
Methods: RT3D-TEE was performed in 52 FMR patients and 30 controls. Mitral annulus dimensions and leaflets tenting were measured throughout systole (TomTec, Germany). Phasic EROA was measured by proximal isovelocity surface area (PISA) method.
Results: Mitral annulus had the minimal area and an oval shape with saddle configuration during early systole in controls, which enlarged and became round and flattened towards mid and late systole ($P < 0.05$). In contrast, annulus in FMR was significantly larger, rounder and flatter ($P < 0.001$), which further dilated and became more flattened at late systole ($P < 0.05$ vs control). Leaflet tenting height in FMR decreased in mid systole and remains unchanged towards late systole. The leaflet tenting volume peaked at early and late systole with a mid-systolic trough in both FMR and controls. But tenting volume of patients with FMR was significantly larger than that of controls (all $P < 0.001$ vs control in whole systole). Further analysis demonstrated that early tenting volume (β value $= 0.053$, $P < 0.05$) was a predictor of early EROA, whereas late tenting volume (β value $= 0.031$, $P < 0.05$) and late annular displacement velocity were predictors of late EROA.
Conclusions: The early and late peak EROAs of FMR was primarily contributed by tenting volume at early systole and late systole respectively. These findings would be of value to consider in interventions aimed at reducing the severity of FMR.

1. Introduction

Functional mitral regurgitation (FMR) is a common finding in patients with chronic left ventricular (LV) systolic dysfunction and is associated with poor prognosis [1,2]. Published data has demonstrated that in patients with LV systolic dysfunction and FMR, a biphasic pattern was observed in instantaneous regurgitant flow rate and effective regurgitant orifice area (EROA) change, including early- and late-systolic peaks with a mid-systolic decrease [3–5] as measured by proximal isovelocity surface area (PISA) method with Doppler echocardiography. Moreover, based on a series of in vitro [6], animal [7], and human [8,9] studies on the mechanism of FMR, we have embraced the concept that pathological tethering and concomitant regurgitation occur when an imbalance is present between closing and tethering forces. Previous studies have mainly applied parameters from 2-dimensional (2D) echocardiography; however, it is well known that mitral valve is a complex three-dimensional structure that could not be accurately assessed using 2D echocardiography. In recent years, real time three-dimensional transesophageal echocardiography (RT3D-TEE) has played increasingly important role in the assessment of mitral valve. The saddle shape of mitral valve can be quantitatively measured with angle, circumference and cubic tenting volume using RT3D-TEE [10]. Although dynamic changes of mitral annulus and phasic

Abbreviations: FMR, functional mitral regurgitation; LV, left ventricle/left ventricular; EROA, effective regurgitant orifice area; PISA, proximal isovelocity surface area; RT3D-TEE, real-time three-dimensional transesophageal echocardiography; MA, mitral annulus/annular; ES, early systole; MS, middle systole; LS, late systole.

* Correspondence author. Tel.: +852 26323140; fax: +852 26373852.
E-mail address: alexpwlee@cuhk.edu.hk (A.P.-W. Lee).

[1] All authors take responsibility for all aspects of the reliability and freedom from bias of the data presented and their discussed interpretation.

http://dx.doi.org/10.1016/j.ijcard.2014.08.001
0167-5273/

mitral regurgitation have been described, there is lack of data regarding the phasic changes of mitral valve geometry estimated with 3-dimensional echocardiography and its relationship to the early- and late-MR. Therefore, we hypothesized that severity of early and late MRs is associated with 3D mitral structural findings in FMR.

2. Methods

2.1. Study populations

A total of 82 subjects including 52 patients with FMR (mean age 68 ± 9 years; 33 males) and 30 controls (mean age 52 ± 14 years; 18 males) were enrolled in this study. FMR was defined as occurrence of MR secondary to regional or global LV dysfunction without intrinsic structural abnormality of the mitral valve. The etiologies of LV dysfunction included prior myocardial infarction, ischemic and/or nonischemic dilated cardiomyopathy. Controls were those who had TEE examination for clinical indications but had no abnormalities confirmed by TEE. All patients were in sinus rhythm and had (1) structurally normal mitral valves, (2) technically adequate color-flow Doppler images for PISA measurement, (3) adequate RT3D-TEE images of the LV chamber and the mitral apparatus to allow off-line analysis. Exclusion criteria were contraindications to TEE, primary heart valve disease, congenital and pericardial diseases, hypertrophic or infiltrative cardiomyopathy, and recent myocardial infarction within 2 weeks.

2.2. Conventional echocardiography

2D/Doppler transthoracic and TEE were performed in all subjects (iE33, Philips, Andover, Mass). LV volumes (end-diastole and end-systole) and ejection fraction were calculated according to the American Society of Echocardiography recommendations [11]. FMR severity was quantified by measuring the EROA using the PISA method [12]. Color and continuous-wave Doppler for EROA were measured at early systole (ES), mid systole (MS) and late systole (LS), using the equation: $EROA_t = 2\pi r^2 \times$ aliasing velocity / $Velocity_t$ respectively, where t = timing in systole. ES was defined as the frame just after closure of the mitral valve; LS was defined as the frame just before the opening of the mitral valve; MS was defined as the middle frame between ES and LS. Severe FMR was defined as mean EROA ≥ 0.2 cm^2 [12].

2.3. Real-time three-dimensional echocardiography

RT3D-TEE was performed using an iE33 ultrasound system (Philips Healthcare, Andover, Mass), equipped with a fully sampled matrix transducer (X7-2t). Gain settings were optimized using the full-volume acquisition mode (60° × 60°) with ECG gating. RT3D-TEE images of the entire mitral valve complex including the mitral annulus, leaflets, papillary muscles and aortic valve were then acquired over 4 consecutive beats, with frame rate between 18 and 36 Hz.

2.4. Three-dimensional mitral valve dynamic parameters measurement

Dynamic analysis of the anatomical structures of the mitral valve, annulus and the closure line of the two leaflets throughout the systole were performed using 4D MV-assessment 2.0 software (TomTec Imaging Systems GmbH, Munich, Germany). The automated tracking workflow delivered the quantitative parameters listed below (Fig. 1):

- Anteroposterior (AP) diameter was defined as the distance between anterior (A) point and posterior (P) point;
- Anterolateral–posteromedial (AL–PM) diameter was defined as the longest distance between two points on the annulus that are derived by intersecting the annulus and a line perpendicular to AP;
- Ellipticity index was defined as ratio of AP to AL–PM;
- MA circumference (3D) was defined as the real length of annulus expanded;
- MA area (3D) was defined as the size of the real area;
- MA area (2D) was defined as the size of area derived by projected area of the 3D MA area;
- MA area 2D/3D was defined as the ratio of annular 2D area to annular 3D area;
- Non-planar angle was defined as the angle between anterior (A) point, the lowest coaptation point and posterior (P) point;
- Tenting volume was defined as the volume enclosed between the nonplanar mitral annulus and the mitral leaflets in 3D space.
- Tenting height was defined as the perpendicular distance between AP and the lowest point of the closure line to LV apex.
- MA displacement was defined as the longitudinal movement of annular centroid.

MA displacement velocity was defined as the first derivative of annular displacement.

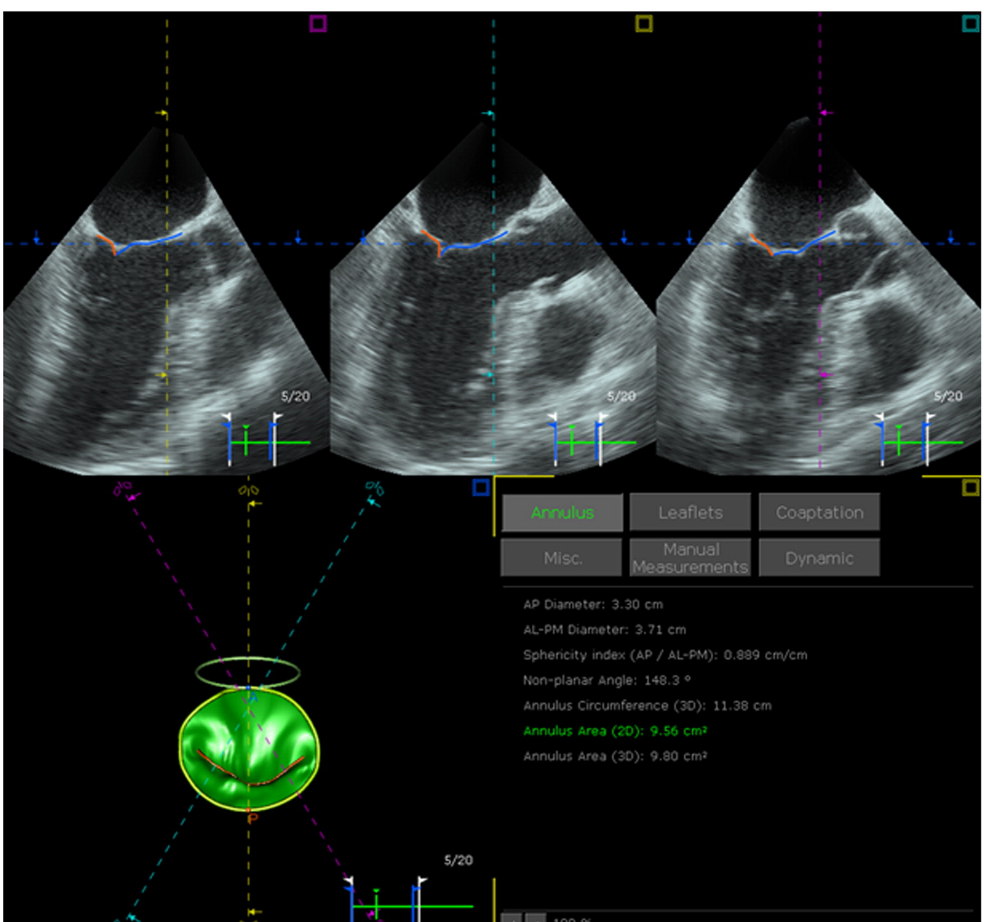

Fig. 1. The automatic tracked and reconstructed of mitral valve.

Please cite this article as: Lin Q, et al, Dynamic assessment of the changing geometry of the mitral apparatus in 3D could stratify abnormalities in functional mitral regurg..., Int J Cardiol (2014), http://dx.doi.org/10.1016/j.ijcard.2014.08.001

2.5. Reproducibility

Reproducibility of the 3D measurements was assessed in 10 randomly selected FMR patients and 10 normal controls. Intra-observer variability was assessed using repeated measurements performed by the same observer 7 days later, while inter-observer variability was evaluated by repeating the analysis by a second independent observer after being trained by the first observer on using the analysis software. Variability was expressed in terms of coefficients of variation between repeated measurements by intra-class correlation coefficient (ICC).

2.6. Statistical analysis

Data are expressed as mean ± SD or number of patients (percentages). Normality of all continuous data was tested with the Kolmogorov–Smirnov test. Intergroup comparisons of mitral valve geometry at early different time points of systole were performed using ANOVA of repeated measures. Within-group comparisons at different time points were performed using paired t test. Chi-square test and the independent Student's t test were performed for intergroup comparisons as appropriate. Univariate and multivariate linear regressions were used to examine for independent predictors of instantaneous EROA at ES and LS. Data were analyzed by dedicated software (SPSS version 17.0, SPSS Inc., Chicago, Illinois, United States). A p-value < 0.05 was considered statistically significant.

3. Results

3.1. Patient characteristics

Patient characteristics and hemodynamic data of all study subjects are listed in Table 1. Compared to controls (n = 30), FMR patients (n = 52) were older with a lower systemic blood pressure (all p < 0.05) although there were no differences in gender distribution, heart rate and body surface area. LV end-diastolic and end-systolic volumes were larger with a lower ejection fraction in patients with FMR than normal controls (all P < 0.05). In the FMR group, 46% had severe FMR with mean EROA = 0.20 ± 0.11 cm^2.

3.2. Comparison of the mitral valve dynamics between functional mitral regurgitation and controls

Table 2 showed the mitral annular dimensions and tenting variables at early, mid, and late systole. In both FMR and normal controls, the AP, AL–PM and ellipticity index increased from ES to MS, and reached their maximum at LS. Compared to normal controls, AP, AL–PM and ellipticity index were larger in FMR throughout systole (all P < 0.001). However, in the FMR group, there was less change of these parameters during systole except for the ellipticity index, which was similar in ES and MS, then increased to its maximum at LS, and was significantly larger (i.e. rounder) than that of the control group at LS (0.95 ± 0.06 vs 0.89 ± 0.06, P < 0.001).

Compared to control subjects, both mitral annular circumference and area were significantly larger in the FMR group throughout systole (P < 0.001). In the control group, annular circumference and area at MS and LS were larger than those at ES (both P < 0.05 for ES vs MS and ES vs

Table 1
Participant characteristics.

Variable	Normal (n = 30)	FMR (n = 52)	P value
Clinical			
Age, y	52 ± 14	68 ± 9	<0.005
Males, n (%)	18 (60%)	33 (63%)	NS
Body surface area, m^2	1.70 ± 0.16	1.65 ± 0.17	NS
Heart rate, beat/minute	76 ± 13	77 ± 15	NS
Systolic blood pressure, mm Hg	140 ± 20	126 ± 23	0.004
Diastolic blood pressure, mm Hg	80 ± 17	72 ± 13	0.034
NYHA class, n (%)			
I	30 (100)	7 (13)	<0.001
II	0 (0)	18 (35)	<0.001
III/IV	0 (0)	27 (52)	<0.001
Echocardiography			
Left ventricle			
Ejection fraction, %	62 ± 5	42 ± 10	<0.005
End-diastolic volume, ml	76 ± 21	125 ± 38	<0.005
End-systolic volume, ml	29 ± 9	73 ± 30	<0.005
Mitral regurgitation			
Mean EROA, cm^2	0 ± 0	0.20 ± 0.11	<0.001
Severe FMR (mean EROA ≥ 0.20 cm^2)	0 (0)	23 (44)	<0.001

EROA indicates effective regurgitant orifice area; NYHA, New York Heart Association.
Values are expressed as mean ± SD or n (%) when appropriate.

Table 2
Three-dimensional mitral valve dynamics in normal controls and FMR patients.

	Normal (n = 30)	FMR (n = 52)	Intergroup P value
Annulus variables			
Anteroposterior diameter (AP), mm			
ES	25.3 ± 2.6*	33.0 ± 4.3*	<0.001
MS	29.3 ± 2.5	34.2 ± 3.9	<0.001
LS	31.1 ± 2.6	36.0 ± 3.9	<0.001
Anterolaterior–posteromedial diameter (AL–PM), mm			
ES	30.6 ± 3.5*	37.2 ± 4.2*	<0.001
MS	34.0 ± 3.0	37.7 ± 3.8	<0.001
LS	35.1 ± 3.3	38.1 ± 3.7	0.003
Ellipticity index			
ES	0.83 ± 0.06*	0.89 ± 0.07*	<0.001
MS	0.87 ± 0.05	0.91 ± 0.06	0.002
LS	0.89 ± 0.06	0.95 ± 0.06	<0.001
Nonplanar angle, °			
ES	140.9 ± 11.9*	152.9 ± 10.6‡	<0.001
MS	141.5 ± 9.7	154.9 ± 17.0	<0.001
LS	144.0 ± 11.5	155.4 ± 9.1	<0.001
Annular circumference, mm			
ES	94.9 ± 10.1*	117.6 ± 12.7‡	<0.001
MS	105.2 ± 9.3	117.8 ± 12.7‡	<0.001
LS	109.1 ± 9.9	121.1 ± 11.2†	<0.001
Annular 2D area, cm^2			
ES	6.3 ± 1.2*	10.2 ± 2.3*	<0.001
MS	7.9 ± 1.3	10.4 ± 2.1	<0.001
LS	8.7 ± 1.5	10.9 ± 2.1	<0.001
Annular 3D area, cm^2			
ES	6.5 ± 1.3*	10.4 ± 2.3*	<0.001
MS	8.2 ± 1.4	10.7 ± 2.1	<0.001
LS	8.9 ± 1.5	11.1 ± 2.1	<0.001
Annular area 2D/3D ratio			
ES	0.960 ± 0.018*	0.977 ± 0.011	<0.001
MS	0.966 ± 0.011	0.977 ± 0.010	<0.001
LS	0.970 ± 0.013	0.979 ± 0.008	0.003
Leaflet tenting variables			
Tenting height, mm			
ES	8.3 ± 1.9*	11.3 ± 2.2†‡	<0.001
MS	6.8 ± 1.9	9.9 ± 2.4	<0.001
LS	7.3 ± 2.0	9.9 ± 2.6	<0.001
Tenting volume, ml			
ES	2.00 ± 0.73†	4.67 ± 1.60*	<0.001
MS	1.62 ± 0.64‡	3.68 ± 1.50	<0.001
LS	2.14 ± 0.89†	4.25 ± 1.74	<0.001
Annulus dynamic variables			
Annular displacement, mm			
ES	0*	0*	N
MS	5.41 ± 1.39	3.29 ± 1.34	<0.001
LS	8.66 ± 1.79	6.19 ± 2.42	<0.001
Annular displacement velocity, mm/s			
ES	20.9 ± 14.4*	16.5 ± 11.4†	0.161
MS	29.5 ± 7.6	22.6 ± 10.0‡	0.001
LS	12.8 ± 5.8	16.9 ± 9.4†	0.054
Mitral regurgitation dynamic variables			
EROA, cm^2			
ES	0	0.29 ± 0.17*	<0.001
MS	0	0.10 ± 0.07	<0.001
LS	0	0.22 ± 0.14	<0.001

Values are expressed as mean ± SD.
ES, MS and LS indicate early systole, middle systole and late systole respectively.
* P < 0.05 for all intra-group comparisons between ES, MS and LS.
† P < 0.05 for intra-group statistically significant difference vs MS.
‡ P < 0.05 for intra-group statistically significant difference vs LS.

Please cite this article as: Lin Q, et al, Dynamic assessment of the changing geometry of the mitral apparatus in 3D could stratify abnormalities in functional mitral regurg..., Int J Cardiol (2014), http://dx.doi.org/10.1016/j.ijcard.2014.08.001

LS). In FMR, annular circumference was dilated ($P < 0.05$ vs controls) and further increased at late systole ($P < 0.05$ LS vs MS). FMR annular 3D and 2D projected areas increased from ES to MS and LS ($P < 0.05$ LS vs MS vs ES), although the percentage of change was smaller than that observed in control subjects.

Mitral annular nonplanarity was represented by the ratio of mitral annular 2D area to 3D area and non-planar angle. Flattening of the mitral annulus was characterized by increasing area ratio (closer to 1) and non-planar angle (closer to 180°). In control subjects, the annular non-planar angle and 2D/3D area ratio both increased from ES to LS. In patients with FMR, the annular non-planar angle was significantly larger than that in controls at ES and increased further at LS; the 2D/3D annular area ratio was also significantly greater in FMR patients than that in controls, remaining so throughout systole. Hence, compared to the controls, the mitral annulus of patients with FMR was significant more flattened during ES, MS and LS (all $P < 0.005$).

In FMR, both tenting volume and tenting height were significantly larger compared to those in controls (all $P < 0.001$ vs normal). In control subjects, the tenting height was maximum at ES, decreased at MS ($P < 0.05$ vs ES), and increased again at LS ($P < 0.05$ vs MS and ES). The tenting volume of control subjects also showed a biphasic change with bi-modal peaks at ES and LS. In contrast, in patients with FMR, the tenting height was also maximal at ES, then decreased in MS ($P < 0.05$ vs ES) and remained static at LS (P = NS vs MS; $P < 0.05$ vs ES). The tenting volume of FMR patients, however, showed a biphasic pattern with bimodal peaks with a higher peak at ES ($P < 0.05$ vs MS and LS), a lower peak at LS, and a trough at MS (Fig. 2).

Compared to control subjects, the mitral annulus motion of FMR was significantly less dynamic with a smaller annular displacement at MS and LS (all $P < 0.001$). There were no difference in the annular displacement velocity during ES and LS between controls and FMR group (all P = NS), but the annular displacement velocity during MS was significant lower in FMR group (22.6 ± 10.0 mm/s vs 29.5 ± 7.6 mm/s, $P < 0.001$). The EROAs measured by PISA method are presented in Table 2. In FMR, the EROA again demonstrated a biphasic bimodal change ($EROA_{ES} = 0.29 \pm 0.17$ cm^2, $EROA_{MS} = 0.10 \pm 0.07$ cm^2 and $EROA_{LS} = 0.22 \pm 0.14$ cm^2, all $P < 0.05$) (Fig. 3), parallel to the change in tenting volume.

3.3. Determinants of early- and late-EROAs

Univariate predictors of $EROA_{ES}$ included ES annular 3D area, non-planar angle, and tenting volume. Multivariate analysis identified only ES tenting volume [$\beta = 0.053$, 95% confidence interval (CI) = 0.009 to 0.096, $P < 0.05$] as independent predictor of $EROA_{ES}$. LS annular 3D area, tenting volume and annular displacement velocity were univariate predictors of $EROA_{LS}$. On multivariate analysis, only tenting volume ($\beta = 0.031$, 95% CI = 0.003 to 0.099, $P < 0.05$) and annular displacement velocity ($\beta = 0.008$, 95% CI = 0.002 to 0.013, $P < 0.05$) were independent predictors of $EROA_{LS}$. (See Tables 3 and 4.)

3.4. Inter- and intra-observer variabilities

Intra- and inter-observer reproducibilities for the measurement of 3D mitral valve parameters were excellent with ICCs ranging from 0.93 to 0.99 and from 0.83 to 0.97 respectively (Table 5).

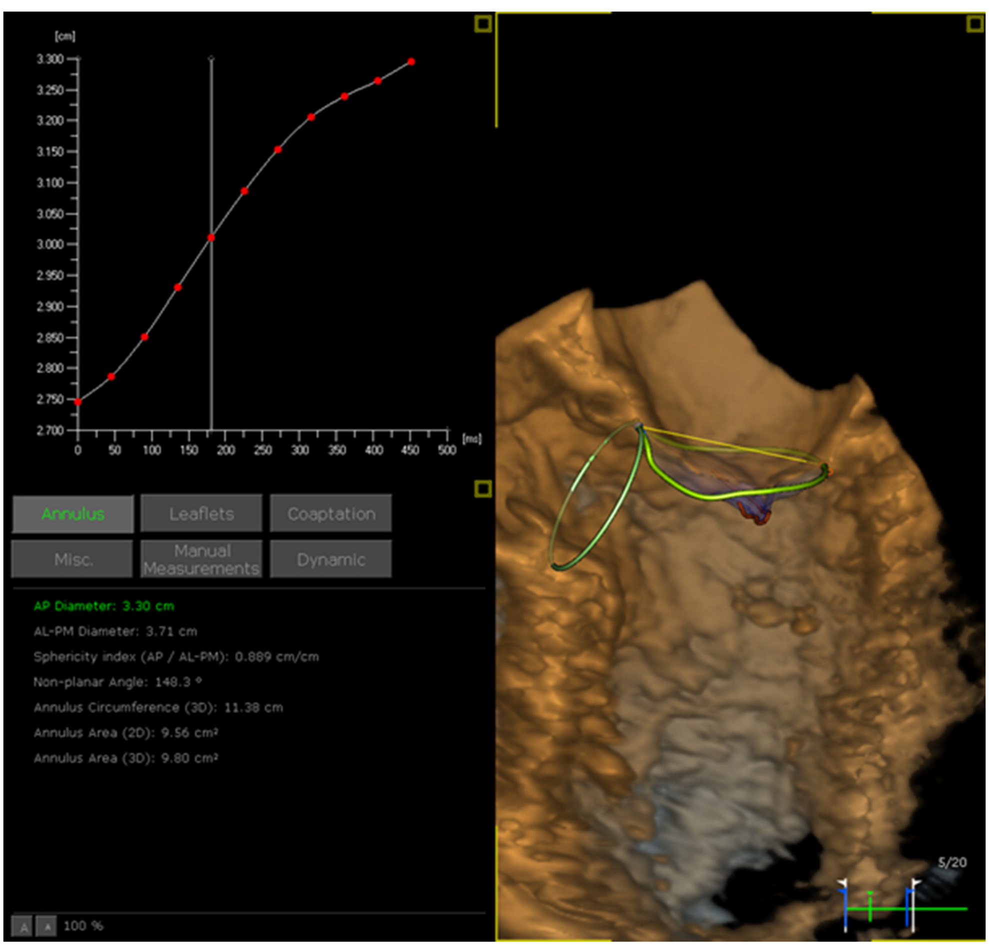

Fig. 2. The tracked result with dynamic parameter changes.

Please cite this article as: Lin Q, et al, Dynamic assessment of the changing geometry of the mitral apparatus in 3D could stratify abnormalities in functional mitral regurg..., Int J Cardiol (2014), http://dx.doi.org/10.1016/j.ijcard.2014.08.001

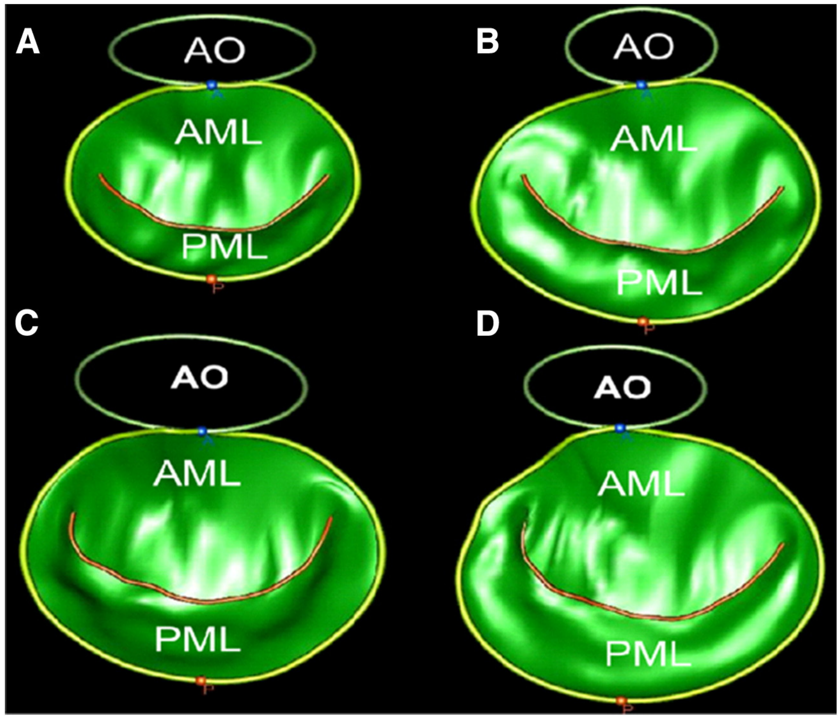

Fig. 3. Dynamic change of mitral valve at systole in control and FMR. A panel: control mitral valve at ES in control group; B panel: mitral valve at LS in control group; C panel: FMR mitral valve at ES; D panel: FMR mitral valve at LS.

4. Discussion

In this study, we demonstrated phasic changes of mitral annulus and leaflet tenting geometry during systole in association with phasic changes of the FMR EROA. We observed that phasic changes of annular geometry during systole were relatively adynamic compared to those in control subjects with normal mitral valve, and there was a biphasic bi-modal pattern of change in leaflet tenting volume during systole, parallel to the phasic change of EROA. To the best of our knowledge, this study is the first to demonstrate that both early and late systolic tenting volumes are independent predictors for corresponding instantaneous EROA at early systole and late systole.

4.1. Dynamic mitral annulus changes in functional mitral regurgitation

Geometric changes of the mitral annulus including increased annular area and decreased annular nonplanarity have been observed in FMR in previous studies [13,14]. Our study confirmed that the saddle shape of mitral valve was lost in FMR [15]. Moreover, the loss of dynamic change of the mitral annulus found in our current study further confirmed that flattening of mitral annulus was persistent during systole.

The change in EROA of FMR from early to mid and late systole in patients with LV systolic dysfunction has a bi-modal pattern in both animal and human studies [3,4,16]. Although it has been recognized that imbalance of closing and tethering forces is related to FMR [17], there is no data with regard to 3D geometry determinants of the phasic change of FMR. Geometric parameters associated with the degree of FMR such as tenting height, area, and volume were derived from instantaneous measurements made on 2D echocardiography [18,19]. Unfortunately, these measurements could be inaccurate because of the high variability of scanning planes and regional variation in both mitral annular shape and leaflet tenting as a result of the complex mitral valve structure. It has been demonstrated that RT3D-TEE provides a precise assessment of many quantitative mitral valve parameters including mitral annulus, leaflet volume and anatomy, tethering distances, and tenting volumes [20–23]. These studies observed that instantaneous measurement of tenting volume at mid systole was generally a strong determining factor of the overall FMR severity. Our study provided novel 3D geometric data of the mitral valve at multiple time points to confirm that early and late systolic tenting volumes were strong determining factors of the instantaneous EROA at the corresponding time points of systole. It was previously believed that a late systolic increase in FMR EROA is a result of decreasing leaflet–closing forces at late systole. However, from a geometric point of view, because tenting volume is conical in shape, an increase in tenting volume can be caused by either increase in leaflet tenting height or increase in annular size. Our study shows that leaflet tenting height decreases in mid systole and remains unchanged towards late systole. Therefore, late systolic annular dilation

Table 3
Multivariate analysis for determinants of early EROA.

Variables (early systolic)	Univariate analysis		Multivariate analysis	
	β (95% CI)	P value	β (95% CI)	P value
Ellipticity index	0.393 (−0.327–1.113)	0.278	NA	NS
Nonplanar angle,°	0.002 (−0.002–0.007)	0.009	NA	NS
Annular 3D area, cm^2	0.027 (0.007–0.047)	0.009	NA	NS
Tenting volume, ml	0.051 (0.024–0.077)	0.000	0.053 (0.009–0.096)	0.019
Annular displacement velocity, mm/s	0.001 (−0.004–0.004)	0.976	NA	NS

CI = confidence interval; NA, not applicable; NS, non-significant.

Please cite this article as: Lin Q, et al, Dynamic assessment of the changing geometry of the mitral apparatus in 3D could stratify abnormalities in functional mitral regurg..., Int J Cardiol (2014), http://dx.doi.org/10.1016/j.ijcard.2014.08.001

Table 4
Multivariate analysis for determinants of late EROA.

Variables (late systolic)	Univariate analysis		Multivariate analysis	
	β (95% CI)	P value	β (95% CI)	P value
Ellipticity index	−0.005 (−0.687–0.675)	0.988	NA	NS
Nonplanar angle,°	0.003 (−0.001–0.007)	0.153	NA	NS
Annular 3D area, cm^2	0.030 (0.013–0.047)	0.001	NA	NS
Tenting volume, ml	0.036 (0.016–0.057)	0.001	0.051 (0.003–0.099)	0.038
Annular displacement velocity, mm/s	0.006 (0.002–0.010)	0.005	0.008 (0.002–0.013)	0.006

CI = confidence interval; NA, not applicable; NS, non-significant.

and flattening rather than re-increase in leaflet tenting towards the end of systole predominantly contributes late systolic increase in the tenting volume.

4.2. Clinical and surgical implications

FMR is common especially in the older populations with heart failure [24]. It is an independent predictor of morbidity and mortality [25]. Even in asymptomatic patients with FMR, nearly half of patients deteriorated with time. Our data suggested that as mechanism of FMR seems to be systolic phase-dependent, evaluation of EROA at different systolic timings may be important for treatment decision. Early systolic FMR may respond better to therapeutic measures that increase LV closing force and reduce leaflet tenting, e.g. inotropes, anti-heart failure medications, and cardiac resynchronization therapy. Late systolic FMR may be more responsive to treatment that prevents or corrects late systolic annular dilatation, e.g. undersized annuloplasty. Since patients with FMR are having a flatter and larger annulus and significantly larger tenting volume, it is reasonable to perform surgical mitral ring annuloplasty with a down sizing rigid saddle shape ring to restore its annulus shape. With saddle shape annulus, it was proposed that the pressure on mitral leaflets is more evenly distributed, imposes less pressure to the native or artificial chordae and renders a more durable mitral repair [26,27].

5. Conclusion

RT3D-TEE is able to quantify dynamic changes of the mitral valve including tenting volume which is related to the biphasic pattern of EROA in FMR. The early peak EROA of FMR was contributed by tenting volume at early systole; similarly, the late peak EROA of FMR was determined by leaflet tenting volume at late systole. These findings would be of value to consider in interventions aimed at reducing the severity of FMR.

Table 5
Intraobserver and interobserver variabilities of 3D measurements.

Variables	Intraclass correlation coefficient (ICC) (95% CI)	
	Intraobserver	Interobserver
Anteroposterior diameter (AP),mm	0.97 (0.93–0.99)	0.91 (0.78–0.96)
Anterolaterior–posteromedial diameter (AL–PM),mm	0.95 (0.88–0.98)	0.88 (0.71–0.95)
Ellipticity index	0.95 (0.87–0.98)	0.83 (0.57–0.93)
Nonplanar angle, °	0.94 (0.85–0.98)	0.94 (0.86–0.98)
Annular circumference, mm	0.96 (0.89–0.98)	0.91 (0.78–0.97)
Annular 2D area, cm^2	0.97 (0.93–0.99)	0.94 (0.84–0.97)
Annular 3D area, cm^2	0.97 (0.92–0.99)	0.93 (0.82–0.97)
Tenting height, mm	0.95 (0.88–0.98)	0.93 (0.83–0.97)
Tenting volume, ml	0.99 (0.97–0.995)	0.97 (0.92–0.99)
Annular displacement, mm	0.94 (0.85–0.98)	0.97 (0.92–0.99)
Annular displacement velocity, mm/s	0.93 (0.83–0.97)	0.88 (0.70–0.95)

Conflict of interest

Prof Alex Pui-Wai Lee provides consultancy to Philips Ultrasound, Inc. Dr Ivan Salgo is an employee of Philips Ultrasound, Inc.

Acknowledgment

This work is partially supported by Hong Kong Research Grant Council General Research Fund (Grant Number: 467812).

Dr Jen-Li Looi acknowledges support from the Overseas Fellowship Award from the National Heart Foundation New Zealand.

Dr Fang Fang and Dr Qing-shan Lin are co-first authors. Both contributed equally and significantly to the manuscript.

References

[1] Trichon BH, Felker GM, Shaw LK, Cabell CH, O'Connor CM. Relation of frequency and severity of mitral regurgitation to survival among patients with left ventricular systolic dysfunction and heart failure. Am J Cardiol 2003;91:538–43.

[2] Koelling TM, Aaronson KD, Cody RJ, Bach DS, Armstrong WF. Prognostic significance of mitral regurgitation and tricuspid regurgitation in patients with left ventricular systolic dysfunction. Am Heart J 2002;144:524–9.

[3] Hung J, Otsuji Y, Handschumacher MD, Schwammenthal E, Levine RA. Mechanism of dynamic regurgitant orifice area variation in functional mitral regurgitation: physiologic insights from the proximal flow convergence technique. J Am Coll Cardiol 1999;33:538–45.

[4] Schwammenthal E, Chen C, Benning F, Block M, Breithardt G, Levine RA. Dynamics of mitral regurgitant flow and orifice area. Physiologic application of the proximal flow convergence method: clinical data and experimental testing. Circulation 1994;90:307–22.

[5] Fukuda S, Grimm R, Song JM, et al. Electrical conduction disturbance effects on dynamic changes of functional mitral regurgitation. J Am Coll Cardiol 2005;46:2270–6.

[6] He S, Fontaine AA, Schwammenthal E, Yoganathan AP, Levine RA. Integrated mechanism for functional mitral regurgitation: leaflet restriction versus coapting force: in vitro studies. Circulation 1997;96:1826–34.

[7] Tibayan FA, Rodriguez F, Zasio MK, et al. Geometric distortions of the mitral valvular: ventricular complex in chronic ischemic mitral regurgitation. Circulation 2003;108: II–116 (Suppl.).

[8] Yiu SF, Enriquez-Sarano M, Tribouilloy C, Seward JB, Tajik AJ. Determinants of the degree of functional mitral regurgitation in patients with systolic left ventricular dysfunction: a quantitative clinical study. Circulation 2000;102:1400–6.

[9] Lee AP, Acker M, Kubo SH, et al. Mechanisms of recurrent functional mitral regurgitation after mitral valve repair in nonischemic dilated cardiomyopathy: importance of distal anterior leaflet tethering. Circulation 2009;119:2606–14.

[10] Lee AP, Hsiung MC, Salgo IS, et al. Quantitative analysis of mitral valve morphology in mitral valve prolapse with real-time 3-dimensional echocardiography: importance of annular saddle shape in the pathogenesis of mitral regurgitation. Circulation 2013;127:832–41.

[11] Lang RM, Bierig M, Devereux RB, et al. Recommendations for chamber quantification: a report from the American Society of Echocardiography's Guidelines and Standards Committee and the Chamber Quantification Writing Group, developed in conjunction with the European Association of Echocardiography, a branch of the European Society of Cardiology. J Am Soc Echocardiogr 2005;18:1440–63.

[12] Zoghbi WA, Enriquez-Sarano M, Foster E, et al. Recommendations for evaluation of the severity of native valvular regurgitation with two-dimensional and Doppler echocardiography. J Am Soc Echocardiogr 2003;16:777–802.

[13] Kono T, Sabbah HN, Rosman H, et al. Left ventricular shape is the primary determinant of functional mitral regurgitation in heart failure. J Am Coll Cardiol 1992;20: 1594–8.

[14] Boltwood CM, Tei C, Wong M, et al. Quantitative echocardiography of the mitral complex in dilated cardiomyopathy: the mechanism functional mitral regurgitation. Circulation 1983;68:498–508.

[15] Kaji S, Nasu M, Yamamuro A, et al. Annular geometry in patients with chronic ischemic mitral regurgitation. Three-dimensional magnetic resonance imaging study. Circulation 2005;112(Suppl. I):I409–14.

Please cite this article as: Lin Q, et al, Dynamic assessment of the changing geometry of the mitral apparatus in 3D could stratify abnormalities in functional mitral regurg..., Int J Cardiol (2014), http://dx.doi.org/10.1016/j.ijcard.2014.08.001

[16] Shiota T, Jones M, Teien DE, et al. Dynamic change in mitral regurgitant orifice area: comparison of color Doppler echocardiographic and electromagnetic flowmeter-based methods in a chronic animal model. J Am Coll Cardiol 1995;26:528–36.
[17] Solis J, McCarty D, Levine RA, et al. Mechanism of decrease in mitral regurgitation after cardiac resynchronization therapy: optimization of the force–balance relationship. Circ Cardiovasc Imaging 2009;2:444–50.
[18] Calafiore AM, Gallina S, Di Mauro M, et al. Mitral valve procedure in dilated cardiomyopathy: repair or replacement? Ann Thorac Surg 2001;71:1146–53.
[19] Ciarka A, Braun J, Delgado V, et al. Predictors of mitral regurgitation recurrence in patients with heart failure undergoing mitral valve annuloplasty. Am J Cardiol 2010;106:395–401.
[20] Watanabe N, Ogasawara Y, Yamaura Y, et al. Geometric differences of the mitral valve tenting between anterior and inferior myocardial infarction with significant ischemic mitral regurgitation: quantitation by novel software system with transthoracic real-time three-dimensional echocardiography. J Am Soc Echocardiogr 2006;19:71–5.
[21] Fattouch K, Castrovinci S, Murana G, et al. Multiplane two-dimensional versus real time three-dimensional transesophageal echocardiography in ischemic mitral regurgitation. Echocardiography 2011;28:1125–32.
[22] Song JM, Fukuda S, Kihara T, et al. Value of mitral valve tenting volume determined by real-time three-dimensional echocardiography in patients with functional mitral regurgitation. Am J Cardiol 2006;98:1088–93.
[23] Moustafa SE, Mookadam F, Alharthi M, Kansal M, Bansal RC, Chandrasekaran K. Mitral annular geometry in normal and myxomatous mitral valves: three-dimensional transesophageal echocardiographic quantification. J Heart Valve Dis 2012;21:299–310.
[24] Singh JP, Evans JC, Levy D, et al. Prevalence and clinical determinants of mitral, tricuspid, and aortic regurgitation (the Framingham Heart Study). Am J Cardiol 1999;83:897–902.
[25] Bursi F, Enriquez-Sarano M, Nkomo VT, et al. Heart failure and death after myocardial infarction in the community: the emerging role of mitral regurgitation. Circulation 2005;111:295–301.
[26] Jimenez JH, Soerensen DD, He Z, He S, Yoganathan AP. Effects of a saddle shaped annulus on mitral valve function and chordal force distribution: an in vitro study. Ann Biomed Eng 2003;31:1171–81.
[27] Jimenez JH, Liou SW, Padala M, et al. A saddle-shaped annulus reduces systolic strain on the central region of the mitral valve anterior leaflet. J Thorac Cardiovasc Surg 2007;134:1562–8.

Please cite this article as: Lin Q, et al, Dynamic assessment of the changing geometry of the mitral apparatus in 3D could stratify abnormalities in functional mitral regurg..., Int J Cardiol (2014), http://dx.doi.org/10.1016/j.ijcard.2014.08.001